Langmuir
Letter
pubs.acs.org/Langmuir

Superhydrophobicity of Boron Nitride Nanotubes Grown on Silicon Substrates

Chee Huei Lee,[†] Jaroslaw Drelich,[‡] and Yoke Khin Yap[†,*]

[†]*Department of Physics, Michigan Technological University, 1400 Townsend Drive, Houghton, Michigan 49931, and* [‡]*Department of Materials Science and Engineering, Michigan Technological University, 1400 Townsend Drive, Houghton, Michigan 49931*

Received February 10, 2009. Revised Manuscript Received March 26, 2009

Partially vertical aligned boron nitride nanotubes (BNNTs) on Si substrates are found to be superhydrophobic in contrast to boron nitride (BN) thin films. While the hexagonal-phase BN films are partially wetted by water with advancing contact angle of about 50°, partially vertically aligned BNNTs can achieve superhydrophobic state with advancing water contact angle exceeding 150°. Our results show that the pH value of water does not affect the wetting characteristics of BNNTs. Since BN is chemically inert, resistive to oxidation up to 900 °C, and transparent to visible−UV light, BNNTs could potentially be useful as self-cleaning, transparent, insulating, anticorrosive coatings under rigorous chemical and thermal conditions.

1. Introduction

Highly hydrophobic surfaces and coatings have gained significant research interest since the middle of 1990s[1−3] because of their water repelling, self-cleaning, and antifouling properties.[4,5] Superhydrophobicity is achieved if water contact angle (CA) is larger than 150° and CA hysteresis (or sliding angle) is small, less than 5−10°.[6] In fact, surfaces with high water CAs can be prepared by a careful manipulation of surface topography and structure at micrometer- and nanometer-size scales.[7] It has been achieved through roughening of hydrophobic material,[8] roughening of material which was later coated with hydrophobic polymer[9] or organic monolayer, as well as plasma treatment,[10] deposition,[11] electrospinning,[12] and painting of hydrophobic particles over a substrate of another material. Hydrophobic organic materials such as fluorinated polymers,[13] olefins, fluorohydrocarbons,[10] and silicon-based hydrocarbons[8,14] were frequently used. However, most of these organic materials could not stand high temperatures. Recently, it was shown that superhydrophobic coatings and films can be prepared using small diameter fibers, wires, rods, and tubes.[12,15,16] Several research groups used carbon nanotubes (CNTs),[17−21] TiO_2[22,23] and ZnO[24] nanowires (NWs), or nanorods as building blocks in preparation of coatings with controllable wetting characteristic. Theoretical studies showed that liquid spreading over highly curved surfaces, such as NTs and NWs, differs from that on plan surfaces.[25,26] In general, it is more difficult for liquid to penetrate the coatings made of fibers and posts than porous bulk materials or coatings made of spherical particles. Here we report on superhydrophobic coatings based on insulating and chemically inert boron nitride nanotubes (BNNTs).

BNNTs are structurally similar to CNTs and possess super strong mechanical properties,[27,28] due to the strong sp^2 bonding within their hexagonal networks. Unlike CNTs, which can be semimetallic or semiconducting, BNNTs are always insulating,[29,30] with an electronic band gap of ∼5.9 eV.[31] Moreover, BNNTs are chemically more stable compared to CNTs.[32] They are excellent

*Corresponding author. E-mail: ykyap@mtu.edu.

(1) Miller, J. D.; Veeramasuneni, S.; Drelich, J.; Yalamanchili, M. R.; Yamauchi, G. *Polym. Eng. Sci.* **1996**, *36*, 1849–1855.
(2) Yamauchi, G.; Miller, J. D.; Saito, H.; Takai, K.; Ueda, T.; Takazawa, H.; Yamamoto, H.; Nislhi, S. *Colloids Surf., A: Physicochem. Eng. Aspects* **1996**, *116*, 125–134.
(3) Veeramasuneni, S.; Drelich, J.; Miller, J. D.; Yamauchi, G. *Prog. Org. Coat.* **1997**, *31*, 265–270.
(4) Feng, L.; Li, S.; Li, Y.; Li, H.; Zhang, L.; Zhai, J.; Song, Y.; Liu, B.; Jiang, L.; Zhu, D. *Adv. Mater.* **2002**, *14*, 1857–1860.
(5) Blossey, R. *Nat. Mater.* **2003**, *2*, 301–306.
(6) Sun, T.; Feng, L.; Gao, X.; Jiang, L. *Acc. Chem. Res.* **2005**, *38*, 644–652.
(7) Ma, M.; Hill, R. M. *Curr. Opin. Colloid Interface Sci.* **2006**, *11*, 193–202.
(8) Jin, M.; Feng, X.; Xi, J.; Zhai, J.; Cho, K.; Feng, L.; Jiang, L. *Macromol. Rapid Commun.* **2005**, *26*, 1805–1809.
(9) Shirtcliffe, N. J.; McHale, G.; Newton, M. I.; Perry, C. C. *Langmuir* **2005**, *21*, 937–943.
(10) Kim, S. H.; Kim, J.-H.; Kang, B.-K.; Uhm, H. S. *Langmuir* **2005**, *21*, 12213–12217.
(11) Zhai, L.; Cebeci, F. C.; Cohen, R. E.; Rubner, M. F. *Nano Lett.* **2004**, *4*, 1349–1353.
(12) Ma, M.; Hill, R. M.; Rutledge, G. C. *J. Adhes. Sci. Technol.* **2008**, *22*, 1799–1817.
(13) Morra, M.; Occhiello, E.; Garbassi, F. *Langmuir* **1989**, *5*, 872–876.
(14) Khorasani, M. T.; Mirzadeh, H.; Kermani, Z. *Appl. Surf. Sci.* **2005**, *242*, 339–345.
(15) Feng, L.; Yang, Z.; Zhai, J.; Song, Y.; Liu, B.; Ma, Y.; Yang, Z.; Jiang, L.; Zhu, D. *Angew. Chem., Int. Ed.* **2003**, *42*, 4217–4220.
(16) Feng, X.; Jiang, L. *Adv. Mater.* **2006**, *18*, 3063–3078.
(17) Kakade, B. A.; Pillai, V. K. *J. Phys. Chem. C* **2008**, *112*, 3183–3186.
(18) Kakade, B.; Mehta, R.; Durge, A.; Kulkarni, S.; Pillai, V. *Nano Lett.* **2008**, *8*, 2693–2696.
(19) Zhu, L.; Xiu, Y.; Xu, J.; Tamirisa, P. A.; Hess, D. W.; Wong, C. P. *Langmuir* **2005**, *21*, 11208–11212.
(20) Lau, K. K. S.; Bico, J.; Teo, K. B. K.; Chhowalla, M.; Amaratunga, G. A. J.; Milne, W. I.; McKinley, G. H.; Gleason, K. K. *Nano Lett.* **2003**, *3*, 1701–1705.
(21) Huang, L.; Lau, S. P.; Yang, H. Y.; Leong, E. S. P.; Yu, S. F.; Prawer, S. *J. Phys. Chem. B* **2005**, *109*, 7746–7748.
(22) Lai, Y.; Lin, C.; Wang, H.; Huang, J.; Zhuang, H.; Sun, L. *Electrochem. Commun.* **2008**, *10*, 387–391.
(23) Feng, X.; Zhai, J.; Jiang, L. *Angew. Chem., Int. Ed.* **2005**, *44*, 5115–5118.
(24) Feng, X.; Feng, L.; Jin, M.; Zhai, J.; Jiang, L.; Zhu, D. *J. Am. Chem. Soc.* **2004**, *126*, 62–63.
(25) Neimark, A. V. *J. Adhes. Sci. Technol.* **1999**, *13*, 1137–1154.
(26) McHale, G.; Käb, N. A.; Newton, M. I.; Rowan, S. M. *J. Colloid Interface Sci.* **1997**, *186*, 453–461.
(27) Chopra, N. G.; Zettl, A. *Solid State Commun.* **1998**, *105*, 297–300.
(28) Suryavanshi, A. P.; Yu, M.-F.; Wen, J.; Tang, C.; Bando, Y. *Appl. Phys. Lett.* **2004**, *84*, 2527–2529.
(29) Rubio, A.; Corkill, J. L.; Cohen, M. L. *Phys. Rev. B* **1994**, *49*, 5081–5084.
(30) Blase, X.; Rubio, A.; Louie, S. G.; Cohen, M. L. *Europhys. Lett.* **1994**, *28*, 335–340.
(31) Lee, C. H.; Wang, J.; Kayatsha, V. K.; Huang, J. Y.; Yap, Y. K. *Nanotechnology* **2008**, *19*, 455605.
(32) Chen, Y.; Zou, J.; Campbell, S. J.; Caer, G. L. *Appl. Phys. Lett.* **2004**, *84*, 2430–2432.

thermal conductors,[33] with high resistance to oxidation at elevated temperature, up to 900 °C.[32,34]

Even though the intrinsic properties of individual NTs are of great interest to fundamental research and important in manufacturing nanodevices,[35] assembly of BNNTs also opens new applications. With our recent capability of depositing long and dense BNNTs on substrates, we have tested the macroscopic wetting characteristic of BNNT coatings. As shown later in this paper, coatings of BNNTs, deposited on silicon substrates, exhibit water repellency, some of which exhibit wetting characteristics typical for superhydrophobic films. Since boron nitride (BN) is a chemically inert and insulating material,[36] it has the potential to serve as a unique protective film for high performance applications. Additionally, turning BN into a superhydrophobic structure opens the prospect of using it as a dry and self-cleaning coating. To our knowledge, no literature has been published on the wettability of BNNT films. The superhydrophobic state of BNNTs has been achieved in spite of the fact that BN thin films are poor hydrophobic materials, with a water CA of about 50°.

2. Experimental Procedures

2.1. Synthesis of BNNTs Films. Synthesis of BNNTs is technically more challenging compared to that of CNTs because of their biatomic nature. Growth techniques of BNNTs include laser ablation/vaporization,[37] arc discharge,[38] ball-milling,[39] CNTs substitution reaction,[40] and chemical vapor deposition (CVD).[41,42] In addition to the problems of contamination, it is challenging to use these techniques to grow arrays of BNNTs on substrates. Recently, we have reported the first success of growing pure BNNTs directly on substrates by plasma-enhanced pulsed-laser deposition (PLD).[43] However, the growth rates of these BNNTs are still low. More recently, dense and long BNNTs have been successfully synthesized in our laboratory by a relatively simple thermal-CVD technique in a conventional tube furnace.[31] This success has enabled the investigation presented in this paper. In brief, B, MgO, and FeO precursors were heated up to 1200 °C to form B_2O_2 reactive vapor. In a NH_3 environment, BN vapor was produced, which condensed on catalyst particles to facilitate the growth of BNNTs.[31] All BNNTs films used in this work were deposited on silicon substrates. No effort was made to remove the native oxide layers on our substrates. Coatings of BNNTs used were obtained after about 1 h of deposition process. The typical length of the tubes was more than 10 μm, whereas the diameter of the tubes ranged from 20 to 60 nm.

2.2. Synthesis of BN Films. BN thin films were deposited by PLD, using a Nd:YAG laser with the fourth harmonic generation (wavelength = 266 nm, pulse duration = 5 ns). The deposition was conducted at 500 °C in a vacuum condition of $\sim 8 \times 10^{-5}$ mbar for 4 h. A hot-pressed h-BN target was used, and the laser energy was recorded to be ~15 mJ/pulse.

2.3. Contact Angle Measurements. The CA measurements were conducted by a sessile drop method according to methodology presented earlier.[44] A Kruss-G10 goniometer with drop shape analysis software was used for measuring both advancing and receding (static) CAs of water. All measurements were carried out using deionized water in ambient environment, at room temperature (~23 °C) and a relative humidity of ~45%. In selected experiments, the pH value of the liquid was adjusted with either diluted NaOH or HCl. A water droplet with a volume of about 10 μL was attached to the substrate by a microsyringe. Small portions of water were added to increase the volume of the drop and reinforce the expansion of the drop base. The advancing CA measurement was carried out 10−20 s after the increase in the diameter of the drop base. Then the needle was immersed into the drop, and water was sucked out by the syringe until noticeable contraction of the drop base was observed. The needle was removed from the drop, and the receding CA was measured 10−20 s after the reduction in drop base diameter. At least five different measurements of both advancing and receding CAs at different locations of the same sample were carried out. In this paper, average values and standard deviations are reported.

2.4. Characterization Techniques. Scanning electron microscopy (SEM) images were obtained with a Hitachi S-4700 field emission scanning electron microscope using 5 kV accelerating voltage and a 7.5−12 mm working distance. A topographical image of BN film was obtained using the intermittent contact mode of operation on a Digital Instruments Dimension 3000 atomic force microscope (AFM). The silicon cantilevers Tap300Al (force constant ~40 N/m, resonant frequency ~300 Hz) from Budget Sensors, with tip radius less than 10 nm (as specified by the manufacturer) were used. Images (5 μm × 5 μm) with 512 × 512 resolutions were captured using a scan rate of 1 Hz. Root-mean-square (rms) and average (R_a) roughness as well as the ratio of measured to projected surface area (r = roughness parameter) were calculated from three images, and average values are presented.

To obtain an estimate of the fractional area of the water droplet in contact with nanotubes (f value) for our samples, a simple image analysis was performed on the captured SEM micrographs, using the MATLAB programming software. In our approach, we assumed that the intensity of the SEM images was mainly corresponding to the depth profile. Therefore, the brightest pixels would be the area where BNNTs contacted a water droplet. The intensity profiles of the SEM images were plotted to calculate the number of pixels, which are above the preset threshold. In each case, the threshold intensity was set to 165.

3. Results and Discussion

3.1. Wettability of Boron Nitride. Water wetting characteristic of BN has not been reported in the literature. Neither single crystal nor large specimen of this material with a flat and smooth macroscopic surface was available to us for measurements of contact angles. In our approach, BN thin films were deposited by PLD as described in the Experimental Procedures. An SEM image and a three-dimensional AFM image of the deposited BN film are shown in Figure 1, along with an optical image of a water drop placed on the surface of this film. The BN thin film deposited on a Si substrate had some particulates, as commonly found in PLD BN films.[45] Despite the particulates, this film had a nominal topography variation at a level of 10−30 nm in vertical direction and 50−80 nm laterally. Roughness

(33) Chang, C. W.; Han, W.-Q.; Zettl, A. *Appl. Phys. Lett*. **2005**, *86*, 173102.
(34) Golberg, D.; Bando, Y.; Kurashima, K.; Sato, T. *Scr. Mater*. **2001**, *44*, 1561–1565.
(35) Yum, K.; Yu, M.-F. *Nano Lett*. **2006**, *6*, 329–333.
(36) Chen, H.; Chen, Y.; Liu, Y.; Fu, L.; Huang, C.; Llewellyn, D. *Chem. Phys. Lett*. **2008**, *463*, 130–133.
(37) Arenal, R.; Stephan, O.; Cochon, J. L.; Loiseau, A. *J. Am. Chem. Soc*. **2007**, *129*, 16183–16189.
(38) Chopra, N. G.; Luyken, R. J.; Cherrey, K.; Crespi, V. H.; Cohen, M. L.; Louie, S. G.; Zettl, A. *Science* **1995**, *269*, 966–967.
(39) Chen, Y.; Chadderton, L. T.; Gerald, J. F.; Williams, J. S. *Appl. Phys. Lett*. **1999**, *74*, 2960–2962.
(40) Han, W.-Q.; Mickelson, W.; Cumings, J.; Zettl, A. *Appl. Phys. Lett*. **2002**, *81*, 1110–1112.
(41) Lourie, O. R.; Jones, C. R.; Bartlett, B. M.; Gibbons, P. C.; Ruoff, R. S.; Buhro, W. E. *Chem. Mater*. **2000**, *12*, 1808–1810.
(42) Zhi, C.; Bando, Y.; Tan, C.; Golberg, D. *Solid State Commun*. **2005**, *135*, 67–70.
(43) Wang, J.; Kayastha, V. K.; Yap, Y. K.; Fan, Z.; Lu, J. G.; Pan, Z.; Ivanov, I. N.; Puretzky, A. A.; Geohegan, D. B. *Nano Lett*. **2005**, *5*, 2528–2532.
(44) Drelich, J.; Miller, J. D.; Good, R. J. *J. Colloid Interface Sci*. **1996**, *179* 37–50.
(45) Wang, J.; Yap, Y. K. *Diam. Relat. Mater*. **2006**, *15*, 444–447.

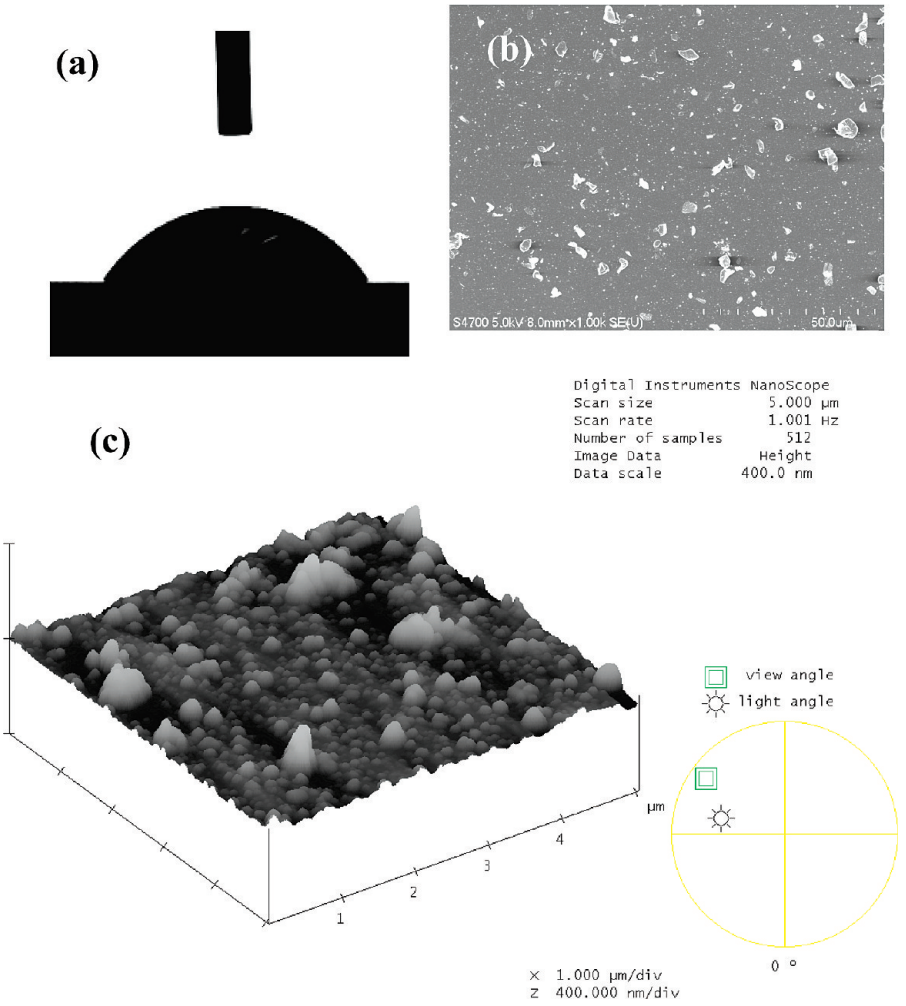

Figure 1. (a) Photograph of a water droplet on a BN thin film. (b,c) FE-SEM image and three-dimensional AFM image of the BN film.

parameters of the BN film determined from the AFM images were as follows: rms = 21.9 ± 1.7 nm, R_a = 14.8 ± 1.3 nm, r = 1.07 ± 0.01.

The advancing water CA measured on the prepared BN film varied from 44° to 52°. The optical image of one of the water drops in advancing mode is shown in Figure 1a. The receding CA was close to zero (less than 10°) and could not be measured with high precision using our goniometer. Both advancing and receding CAs measured on the BN film were most likely influenced by the nanoscaled topography of the surface.[46] To calculate the corresponding contact angles on the smooth surface of BN material, the Wenzel equation was used:[47]

$$\cos(\theta_A)_r = r\cos(\theta_A)_s \quad (1)$$

where $(\theta_A)_s$ and $(\theta_A)_r$ are the advancing CAs on smooth and rough surfaces, respectively.

Equation 1 predicts that the corrected advancing water CA on the BN film with a smooth surface is $(\theta_A)_s$ = 48−55°. These values are only 3−4° larger than advancing CAs measured on the nanoscaled rough surface of the BN film. The CA values indicate that water spreads only partially on the BN surface. Nevertheless, the CAs are small enough to promote capillary penetration of water into a structure of any porous BN material. The capillary penetration inside the structures of nanotubes, on the contrary, is restricted by the effect of high fiber curvature, as is demonstrated in the next part of this contribution.

3.2. Water-Repellent Films of BNNTs. All BNNT samples used in this study had high structural orders and stoichiometric composition (B:N ∼ 1:1), as suggested by the electron energy loss spectroscopy (EELS), Raman spectroscopy, and Fourier transform infrared (FTIR) spectroscopy reported elsewhere.[31]

The CA measurements were conducted on several BNNT films. As shown in Figure 2, BNNT films are significantly more hydrophobic than BN thin films. The advancing water CAs measured for BNNT films, with a value of 145−160°, were consistent with values reported previously for superhydrophobic coatings.[12,48] The receding water CAs measured for selected drops were only 2−5° smaller than the advancing CA (Figure 3), with an average CA hysteresis of about 3.8° for all the samples. However, the effect of drop size on receding CA was sometimes significant, especially when the size of the drop was reduced significantly below the drop size used in the advancing CA measurements; a reduction in the receding CA to less than 90−100° was not uncommon. The effects of surface roughness and heterogeneity on drop size versus CA relationships have been extensively discussed in the literature for other systems.[44,49]

The high value of measured CAs has also led us to investigate the origins of superhydrophobicity of BNNT films. Experiments

(46) Bren, L.; English, L.; Fogarty, J.; Policoro, R.; Zsidi, A.; Vance, J.; Drelich, J.; Istephanous, N.; Rohly, K. *J. Adhes. Sci. Technol.* **2004**, *18*, 1711–1722.
(47) Wenzel, R. N. *Ind. Eng. Chem.* **1936**, *28*, 988–994.
(48) Kim, S. H. *J. Adhes. Sci. Technol.* **2008**, *22*, 235–250.
(49) Drelich, J. *J. Adhes.* **1997**, *63*, 31–51.

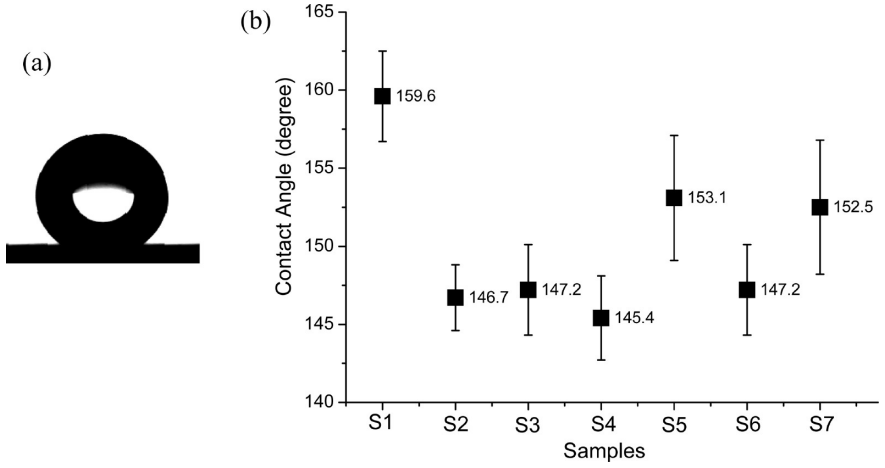

Figure 2. (a) Photograph of a water droplet on a BNNT film. (b) Advancing water CAs measured on seven different films of randomly aligned BNNTs.

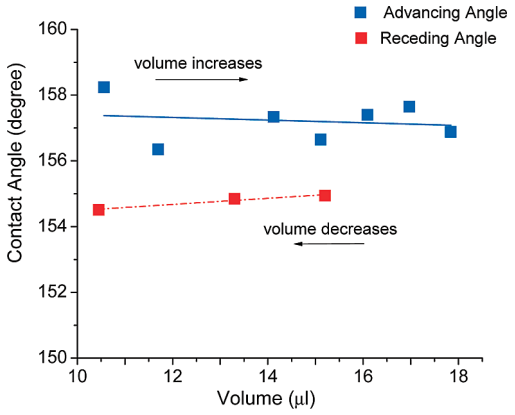

Figure 3. The effect of drop volume on advancing and receding water CAs measured on the BNNT film.

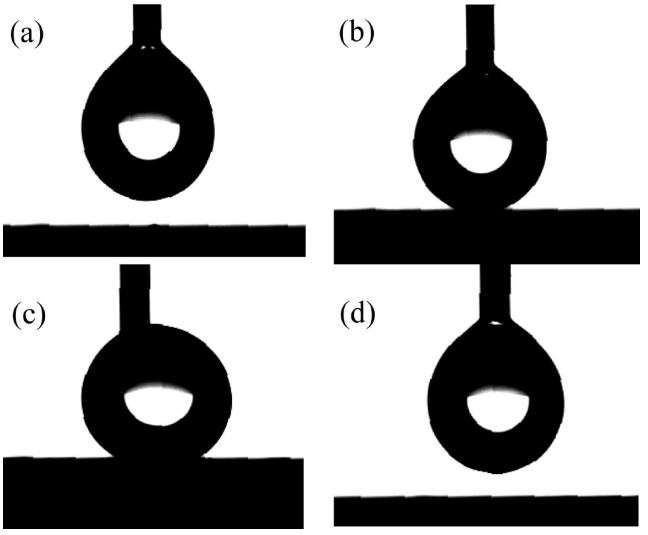

Figure 4. Photographs showing attachment and detachment of a water drop to the BNNT film.

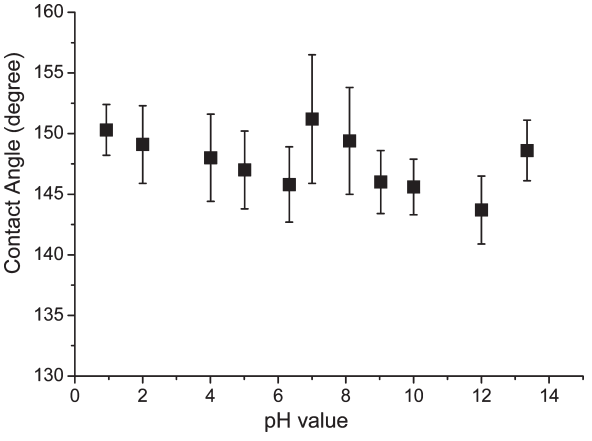

Figure 5. Advancing CAs measured for water of varying pH on the BNNT film.

were carried out by moving the BNNT films toward a suspended droplet (Figure 4a,b), and slowly pushing the sample against the droplet (Figure 4c). Subsequently, the sample was removed from the droplet (Figure 4d). It was found that the suspending droplet was difficult to attach to the BNNT film surface. No visual water residue was left on the sample. This experiment indicated that the adhesion between the BNNT film and the water droplet is much weaker than that between the needle and the water drop. Small drop−BNNT film contact area is expected because of the small diameter of nanotubes and the low packing density of fibers, which is the primary cause for the weak adhesion between the BNNT film and the water drop.

3.3. Effect of pH on the Wettability of BNNT Films. In order to investigate the feasibility of self-protecting BNNT films in both acidic and basic environments, we investigated the influence of pH value of water on measured CAs. As shown in Figure 5, the measured advancing CAs were practically insensitive to the pH of water. Similar to the deionized water case, it was found that both acidic and alkaline solutions remained suspended on the BNNT film as drops instead of penetrating its structure. Also, receding CAs were not affected by the pH of the water (not shown).

The BNNT film was further soaked in a strong HCl solution (~5 M), for more than 36 h. The CA measurements were conducted before and after HCl treatment. As shown in Figure 6, the advancing CA dropped from ~155° to 136°, indicating a reduction in water repellency of the BNNT film. Examination of the BNNT film under SEM revealed that soaking the tubes in acid caused them to clamp into bundles (Figure 6), with no visible structural damages/changes on individual BNNTs. The tubes in the soaked sample were more densely packed than those in the as-grown sample. The bundling is believed to be of similar

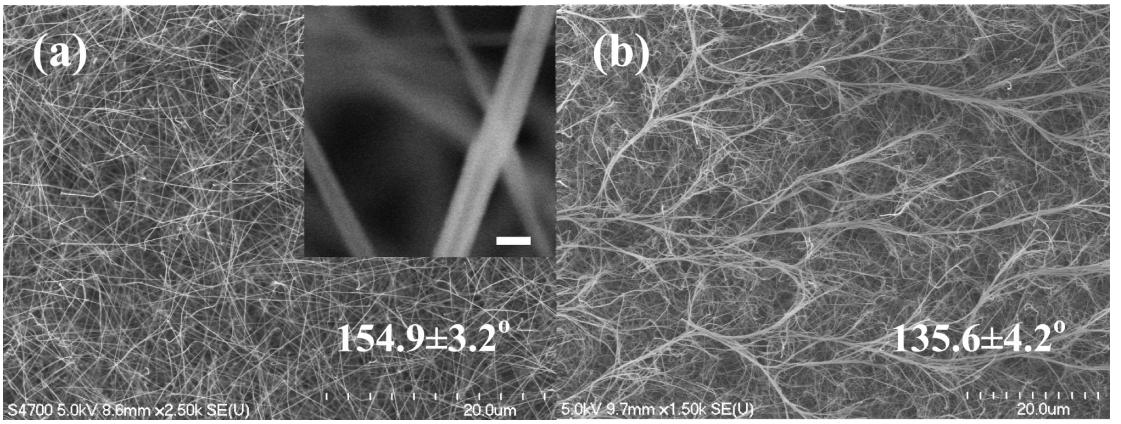

Figure 6. SEM micrographs of a BNNT film (a) before and (b) after acid treatment for ~36 h and advancing water CAs measured for this film. The inset of panel "a" is a high-magnification image, revealing the hollow center channel of the BNNTs. The scale bar is 60 nm.

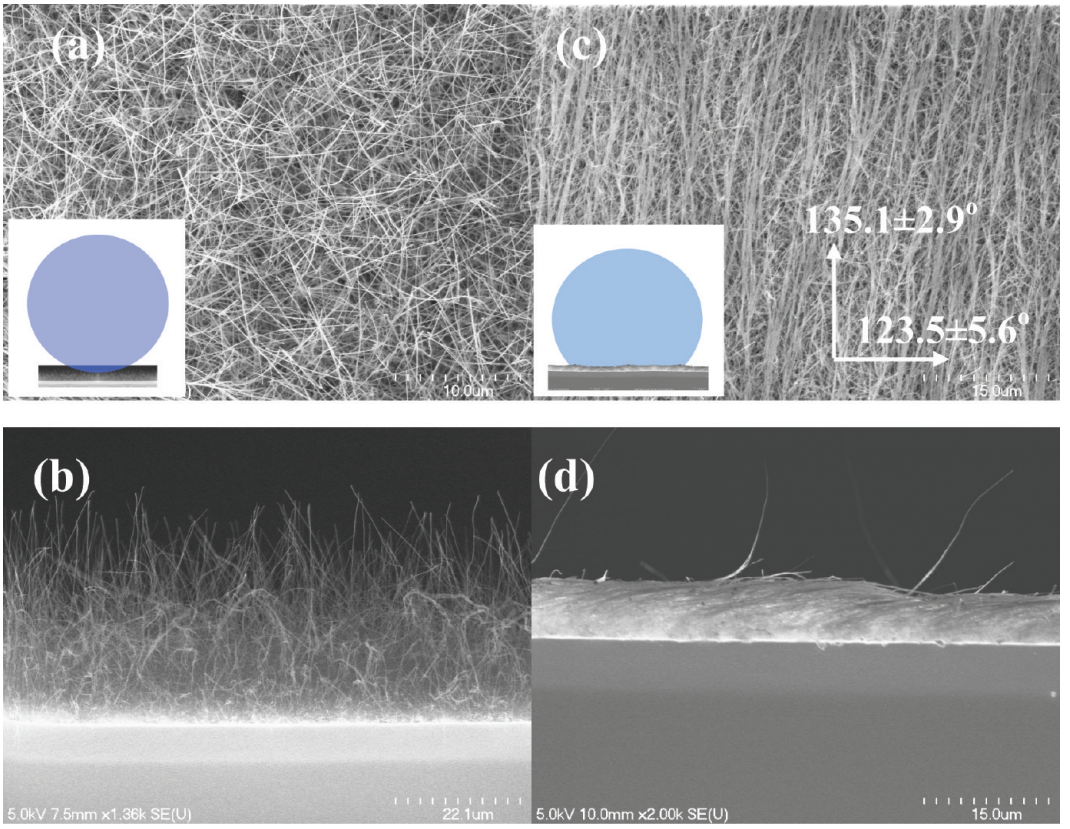

Figure 7. (a) The surface morphology of the as-grown BNNTs on a Si substrate. (b) A cross-sectional view of the as-grown BNNTs. (c) The surface morphology of a BNNT film flattened by a mechanical pressing. (d) A cross-sectional view of the flatten BNNTs.

origin as observed for CNTs by Lau et al.[20] In short, it is the result of attractive capillary forces triggered by residual water left on the film surface that undergoes evaporative drying.[20]

3.4. Water-Repellency of Compressed BNNT Film. We further verified the effect of NT morphology on its wetting characteristic by measuring the CAs on BNNT films with "flattened" structures of tubes. In this experiment, the BNNT film was mechanically pressed against a flat smooth glass slide, causing the tubes to arrange into a flatten configuration. Figure 7a,b shows the top view and cross-sectional view of the as-grown partially vertically aligned BNNTs, respectively, while the images in Figure 7c,d shows the flattened BNNTs. The SEM images indicate a significant difference among the morphologies of both samples. The advancing water CA measured on this flattened BNNT film was determined to be ~135°, which is almost identical to that reported in Figure 6 for the BNNT film soaked with acid. We believe that the bundling phenomenon in both acid-treated and flattened samples increases the number of tubes in contact with the water drop during CA measurements, subsequently reducing the area of drop base in contact with the air pockets formed in between the fibers.

3.5. Image Analysis of BNNTs Films and Correlation with the Cassie−Baxter Equation. We attempted to correlate the measured advancing CAs with the theoretical predictions using the Cassie−Baxter equation:[50]

$$\cos\theta_{\mathrm{BNNTs}} = f(\cos\theta_{\mathrm{BN}} + 1) - 1 \qquad (2)$$

(50) Cassie, A. B. D.; Baxter, S. *Trans. Faraday Soc.* **1944**, *40*, 546–551.

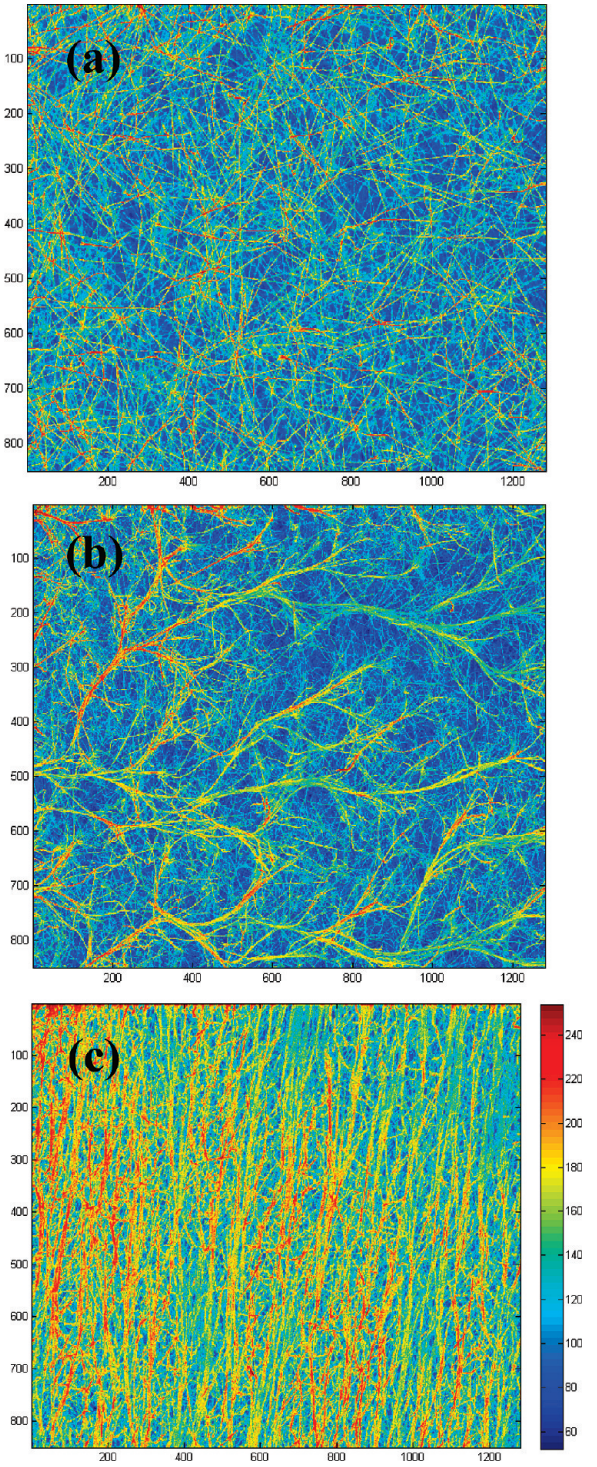

Figure 8. The intensity profile with respect to (a) partially vertically aligned BNNTs (Figure 6a), (b) BNNT film after acid treatment (Figure 6b), and (c) flattened BNNT film (Figure 7b).

where θ_{BNNTs} and θ_{BN} are the contact angles measured on the BNNT film and BN material, respectively, and f is the fractional area of the drop base in contact with the tubes. The f value for eq 2 was determined through image analysis of BNNT films, as described in the Experimental Procedures section. Figure 8 presents the intensity profiles of the SEM images. It was found that the f value of the partially vertically aligned tubes was ~11.9%, while the acid treatment surface and the flattened tubes had f values of 16.2% and 37.0%, respectively. As shown in Table 1, the trend of the water CA is consistent with what the Cassie−Baxter model predicts. We also conclude that the origin of the superhydrophobic properties of the BNNT film is mainly associated with the partially vertical alignment of BNNTs on the Si substrate. Those acid-treated and flattened BNNTs have a tendency to become bundled, and they appear to be laterally more organized, leaving reduced-size openings in between the tubes.

Table 1. Comparison of Water Contact Angles Measured Experimentally and Calculated Theoretically Using the Cassie−Baxter Model

		water CA, θ_{BNNTs}	
samples	f	experimental	calculated (Cassie−Baxter model)
partially vertically aligned BNNTs	0.119	~155 ± 3°	144°
acid-treated BNNTs	0.162	~136 ± 4°	138°
flattened BNNTs	0.370	~135 ± 3°	114°

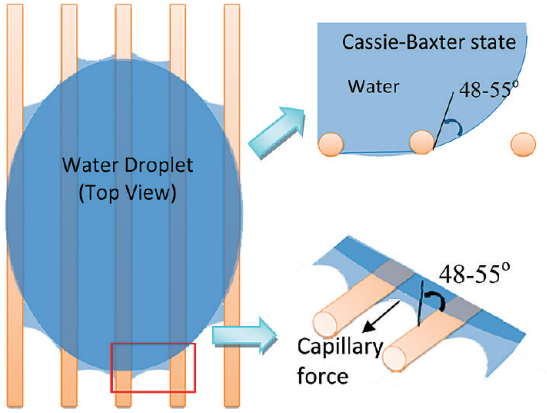

Figure 9. Schematic model of a water droplet placed on laterally aligned BNNTs.

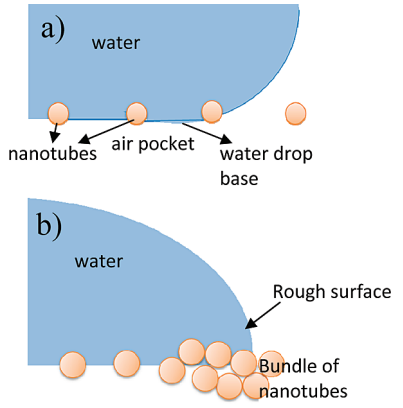

Figure 10. (a) Cassie−Baxter state: water in contact with nanotube−air "composite". (b) Wenzel — Cassie state: water drop base in contact with rough surface formed by nanotubes.

3.6. Wetting Anisotropy of BNNT Films. We noted that laterally aligned tubes demonstrated anisotropy in wetting behavior.[12,51] About 10−15° smaller advancing water CAs were measured on the side of the drop with the baseline crossing the aligned tubes perpendicularly than for the drop baseline situated

(51) Mizukoshi, T.; Matsumoto, H.; Minagawa, M.; Tanioka, A. *J. Appl. Polym. Sci.* **2007**, *103*, 3811–3817.

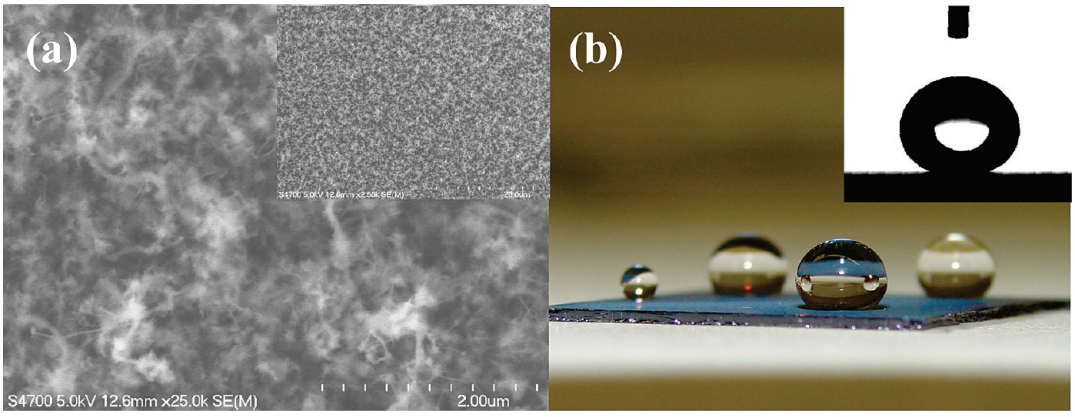

Figure 11. (a) Surface morphology of short BNNTs, forming a thin film. (b) A photograph of water droplets on a sample shows the superhydrophobicity of BNNTs.

along the tubes (Figure 7c). Similar anisotropy was also observed for the acid-treated BNNT film (discussed earlier), although to a smaller extend. The anisotropy in wetting of aligned BN tubes is expected to be the result of capillarity effect. As illustrated in Figure 9, because of the small CA for water on BN material (48−55°), the water meniscus formed between two parallel tubes will tend to stretch the drop base in the direction of the aligned tubes. As the result, the apparent CA measured with the goniometer is smaller than on the side of the drop where this effect is not present.

The difference in contact angles measured on two sides of the drop during experiments with anisotropic BNNT film can also be discussed in terms of the Cassie−Baxter state[52] (for the drop side located along the aligned tubes) and the Wenzel−Cassie state (for drop base crossing the tubes perpendicularly).[53] A water droplet was observed to hardly attach to a BNNT film substrate if the conditions satisfied the Cassie−Baxter state (Figure 10a); the advancing CA up to 160° could be observed as discussed earlier. On the drop side where the Wenzel−Cassie state[54] applies, the water drop base is not only in contact with both tubes and air but also contorted and pinned on a "rough surface" formed by bundled tubes (Figure 10b). At the same time, adhesion of the water drop to bundled BNNTs increased. For example, a ∼10 μL water droplet dropped on the BNNT film surface did not slide easily as in the case of flattened BNNTs, even when the sample was held vertically or turned upside down. The transition from the Cassie−Baxter state to the Wenzel−Cassie state results in the loss of water repellency, important to the state of superhydrophobicity.[53,55]

3.7. Water-Repellency of BNNT Film with Reduced Length of Nanotubes. Finally, we also report the results of CA measurements for a BNNT film sample produced at 1100−1150 °C. The surface morphology of this sample was significantly different than that of dense BNNT films discussed in previous parts of this section. As shown in Figure 11a, short, thin, and irregular BNNTs covered the surface of a Si substrate. The typical diameter and length of the tubes is about 10−40 nm and ∼500 nm, respectively. Although the overall quality and quantity of the tubes are not satisfactory at lower growth temperature, this sample exhibited excellent superhydrophobic behavior. The advancing CA was measured to be 165.5 ± 5.1°. A hysteresis for this sample was determined to be about 5°. In this case, it was even difficult to place a water droplet on the sample. The water sliding angle was less than 5°. Figure 11b shows a photograph of several water droplets on a substrate. We believe that this superhydrophobicity is a result of a more rigid structure of tubes that does not collapse under the weight of the water droplet, compared to BNNT films with longer tubes, therefore producing smaller nanotube−water contact area.

3.8. Future Research. Even though we show the superhydrophobic behavior of BNNT film, water repellency of the structured BNNTs could be improved. For example, it has been recognized that the hierarchical structure is beneficial to enhance the superhydrophobicity of material.[19,56,57] Therefore, engineering BNNTs into a micropatterned surface or pattern of BNNTs grown on a substrate may be feasible for further enhancement of superhydrophobicity of BNNTs structures. Moreover, surfaces of BNNTs could be modified chemically.[21,58] The surface of BNNTs may be functionalized by either hydrophobic nanoparticles[59] or fluorohydrocarbon molecules[19,60] to enhance the hydrophobicity of the material. These approaches are, however, beyond the goal of this contribution, and they will be explored in future research.

4. Conclusions

We discovered that partially vertical aligned BNNT films exhibit strong water repellency, with the advancing water CA exceeding 150° and only a few degrees of CA hysteresis. This is in contrast with BN thin films, which can be partially wetted by water with an advancing CA of about 50°. Our results indicate that the CAs of water droplets on BNNT films can be predicted by the Cassie−Baxter equation. Bundling of nanotubes after mechanical compression or prolonged soaking in acids can increased the number of nanotubes in contact with the water droplets and therefore reduce the advancing contact angles to ∼134−137°. We show that the pH value of water does not affect the wetting characteristic of BNNT films. Since BN is chemically inert and resistive to oxidation up to 900 °C in ambient environment, BNNTs could be useful as a superhydrophobic, self-cleaning,

(52) The Cassie−Baxter state is often called the Cassie state in most of the publications.

(53) Carbone, G.; Mangialardi, L. *Eur. Phys. J. E* **2005**, *16*, 67–76.
(54) Wang, S.; Jiang, L. *Adv. Mater*. **2007**, *19*, 3423–3424.
(55) Quere, D.; Lafuma, A.; Bico, J. *Nanotechnology* **2003**, *14*, 1109–1112.
(56) Nosonovsky, M.; Bhushan, B. *Nano Lett*. **2007**, *7*, 2633–2637.
(57) Nosonovsky, M.; Bhushan, B. *Langmuir* **2008**, *24*, 1525–1533.
(58) Verplanck, N.; Galopin, E.; Camart, J. C.; Thomy, V.; Coffinier, Y.; Boukherroub, R. *Nano Lett*. **2007**, *7*, 813–817.
(59) Zhi, C.; Bando, Y.; Tang, C.; Golberg, D. *J. Phys. Chem. B* **2006**, *110*, 8548–8550.
(60) Jokinen, V.; Sainiemi, L.; Franssila, S. *Adv. Mater*. **2008**, *20*, 3453–3456.

protective and anticorrosive surface under rigorous chemical and thermal conditions. In addition, BNNTs are transparent to visible light.[31] Therefore, the BNNT films could also find applications as a self-cleaning coating on optical devices or lenses, in which high transmission of visible light is desirable.

Acknowledgment. Y.K.Y. is grateful for the support from the National Science Foundation (*CAREER* Award No. 0447555). This project is in part supported by the Department of Energy, the Office of Basic Energy Sciences (Grant No. DE-FG02-06ER46294). Contribution from Derek Mayer is acknowledged here.